JOURNAL OF MATERIALS SCIENCE 24 (1989) 3717–3724

Crystallization and precipitation structures of quasicrystalline phase in rapidly solidified Al–Mn–X ternary alloys

T. OHASHI, N. FUKATSU
Department of Materials Science and Engineering, Nagoya Institute of Technology, Nagoya, Japan

K. ASAI
Daido Steel Co. Ltd, Nishiki 1-11-18, Naka-ku, Nagoya, Japan

Tranmission electron microscopic observations were carried out to reveal the solidification and precipitation structures of rapidly solidified Al–Mn–X alloys (X = Si or Zr), with particular focus on the formation of the icosahedral quasicrystals. On increasing the manganese content, the distribution of the icosahedral quasicrystals in the rapidly solidified alloys changed from the type of cell-boundary segregation to that of one component in the eutectic and the primarily dendritic phase. The precipitation of the icosahedral quasicrystals from the supersaturated solid solutions of the present alloys was restricted in the surface layers and/or large-angle grain boundaries. The orientation relationships between the icosahedral quasicrystals and the aluminium matrix were such that three mutually perpendicular two-fold axes of the icosahedron lie along the [1 0 0], [0 $\bar{1}$ 1], and [0 1 1] axes of the f c c crystallographic directions. The 15-fold symmetry diffraction pattern frequently obtained from (1 1 1) and/or (2 3 3) matrix planes could be explained by considering axial rotation between the five-fold and three-fold symmetry axes of the icosahedron and cubic lattices. It was suggested that the hierarchy of the free energies of the icosahedral phase and the other crystalline phases was very close.

1. Introduction

It is well known that the limiting equilibrium concentration of manganese in aluminium can be extended markedly by rapid solidification [1]. Various metastable precipitates have also been found, namely G [2], G′, and G″ [3]. In addition to these phases, Shechtman *et al.* [4] have reported the presence of a less stable phase, designated T, in rapidly solidified Al–5 wt % Mn foils following short annealing periods. The T phase is now of interest because of the striking resemblance of electron diffraction patterns to those obtained from a quasicrystal [5] having icosahedral point group symmetry, which was first found in the rapidly solidified alloys of Al–18 to 25.3 wt % Mn which were employed in Shechtman *et al.'s* work [6, 7].

In our previous work [8] on the precipitation characteristics of rapidly solidified Al–7 wt % Mn–1 wt % Zr alloys, it has been shown that appreciable precipitation hardening takes place during annealing at temperatures between 623 and 723 K. In these cases, the manganese enhanced the precipitation hardening because the increase in hardening was about twice that of the Al–1 wt % Zr binary alloys [9] under optimum conditions of temperature and manganese content. The results of X-ray diffraction analyses (XRD) and transmission electron microscope (TEM) observations suggested that the principal precipitate contributing to the hardening was a pseudomorphous phase of the equilibrium Al_6Mn.

We, in succession, studied preliminarily the structures of precipitate phases and reported the formation of icosahedral quasicrystals by a nucleation and growth process in the supersaturated solid solutions of the Al–Mn–Zr alloys prepared by melt spinning [10]. Cassada *et al.* [11–14] have also reported the formation of icosahedral phases in Al–Li–Cu, Al–Mg–Cu and Al–Mg–Zn alloys not by rapid solidification, but by solid-state reaction in the process. They revealed that those phases nucleate at high-angle grain boundaries and grow outwards into the matrix. It is very interesting to note that there is an orientational relationship between the icosahedral phase and the aluminium matrix in the Al–Li–Cu ternary alloys [12, 14]. Also in our recent report [10], we examined the orientational relationships between quasicrystalline precipitates and the aluminium matrix by several selected-area diffraction patterns taken from the different zone axes of the matrix grains and proposed that the five-fold and two-fold axes of the icosahedral precipitate were, respectively, put in parallel with ⟨1 1 1⟩ and ⟨0 1 1⟩ zone axes of the matrix. If a still more precise relationship were presented, the $[1\,0\,0\,0\,0\,0]_{\text{icosahedron}}$ is parallel with $[6\,7\,7]_{\text{cubic}}$. This result is in good agreement with the work of Buddai and

0022–2461/89 $03.00 + .12 © *1989 Chapman and Hall Ltd.*

Aziz [15] which was carried out by the observation of solid-phase precipitation of quasicrystals during ion implantation of manganese into a crystalline aluminium matrix. It is pointed out, however, that there are considerable differences in the precipitation morphology, i.e. grain boundary or intergranular precipitation, of the quasicrystals between the above works [14, 15].

This investigation is aimed to clarify the precipitation morphology of the quasicrystals, as well as the others which have been observed at the same time, by employing melt-spun Al–Mn–Zr and Al–Mn–Si alloys.

2. Experimental procedure

The starting materials used in this study were pure aluminium (99.99 wt %), pure manganese (99.9 wt %), and master alloys of Al–10.4 wt % Mn (Fe < 0.12, Si < 0.03 wt %) and Al–5.35 wt % Zr (Fe < 0.15, Si < 0.13 wt %). We prepared several alloy compositions, nominally of Al–7 to 13 wt % Mn–1 wt % Zr and Al–7 to 13 wt % Mn–0.5 to 1.5 wt % Si ternary alloys, and ingots of dimensions of ~150 mm long and 12 mm diameter were made by casting from 1223 K into a massive graphite mould. Segregation of large intermetallic compounds cannot be observed by macroscopic and optical microscopic examinations of the ingots. These ingots were further hot-forged to 7 mm diameter and sectioned to about 30 mm long for rapid solidification. Each of these samples was remelted in a graphite tube nozzle by high-frequency induction current and, using a melt-spinning device in a nitrogen gas atmosphere, the melt stream was ejected nitrogen gas on to a copper rotating wheel, 220 mm diameter. The rotating speed of the wheel was 3600 r.p.m. and gave ribbons of 30 to 50 μm thick and 2 to 3 mm wide. These ribbons were cut to lengths of about 30 mm and then annealed in an oil or salt bath at 623 to 723 K. X-ray diffraction analyses were made to estimate the extent of manganese solubility and to identify precipitates in the alloys. For transmission electron microscopic (TEM) (Jeol 1200EX, 200 kV) observations, specimens were prepared by electrolytic polishing in a methanol–perchloric acid solution while some specimens were directly observed after cleaning their surfaces with acetone and ethanol; here this process is referred to as direct observation.

3. Results and discussion

3.1. Survey of solidification structures bearing quasicrystalline phase

As pointed out previously [1], an Al–Mn alloy is typical of alloys whose solid solubility limits can be extended markedly by rapid solidification, and which produce several metastable phases when the concentration of the solute exceeds its solubility limit [2, 3]. Before, referring to the precipitation morphologies, an examination of the solidification structures containing quasicrystalline phase in the melt-spun alloys containing comparatively lower concentrations of manganese ($\leqslant$ 20 wt %) was carried out by TEM observations.

Figs 1 to 4 show some typical morphologies of icosahedral phases. According to linear lattice parameter change with manganese content the extent of solid solubility could be estimated up to about 10 wt % [8], but considerable amounts of the icosahedral phase appear at cell grain boundaries even in alloys containing less than 10 wt % Mn (Fig. 1a). Thus it seems to be difficult to suppress entirely the segregation of manganese during rapid soldification. Morphologically different types of the icosahedral phases could often be seen in unspecified parts of the same alloys as shown in Fig. 2. They are distributed at random and have a hexagonal or decagonal shape of 0.2 to 0.3 μm diameter. It is interesting to note that projection of two-, three- and five-fold axes of an icosahedron on to a plane makes similar shapes to the above polygons [16]. These icosahedral phases may have been formed as a primary phase in the not-so-undercooled liquid of the alloys during melt spinning. A selected-area diffraction (SAD) pattern taken from these small particles has shown more diffraction spots in a given range of scattering angles compared with the diffraction patterns taken from the icosahedral phase at the grain boundaries (Fig. 1). This pattern

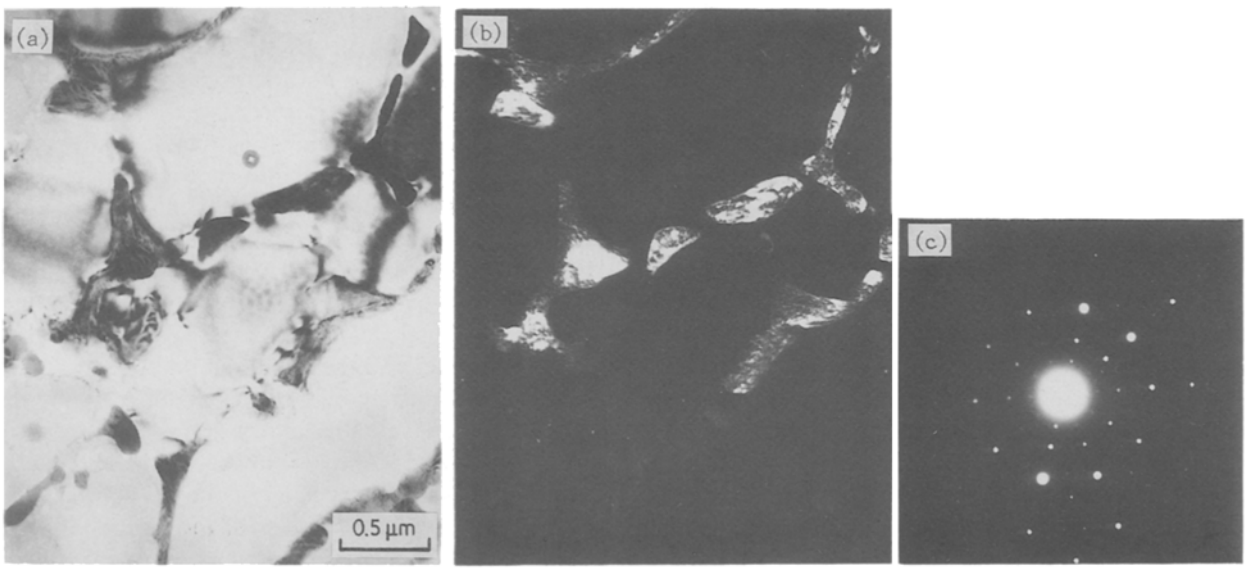

Figure 1 Rapidly solidified structure of Al–7 wt % Mn–0.5 wt % Si alloys, showing segregation of icosahedral quasicrystals at cellular grain boundaries: (a) bright- and (b) dark-field images, and (c) SAD pattern (five-fold symmetry zone).

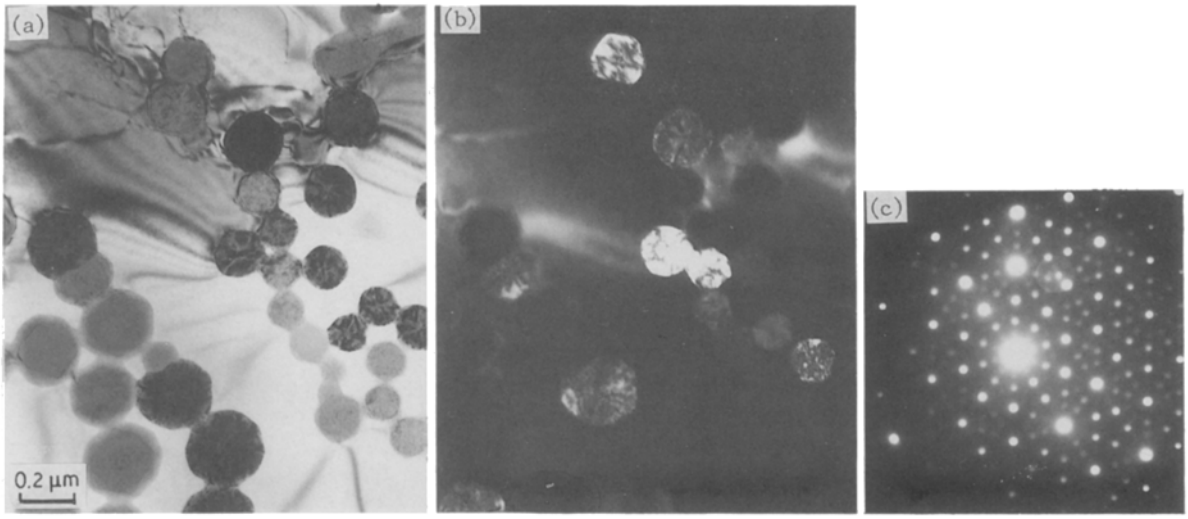

Figure 2 Rapidly solidified structure of the same alloys as in Fig. 1, showing freely dispersed icosahedral quasicrystals: (a) bright- and (b) dark-field images, and (c) SAD pattern (five-fold symmetry zone).

has a close resemblance to that obtained from $Al_{74}Si_6Mn_{20}$ or $Al_{72}Si_6Mn_{22}$ which gives a "superlattice-like" diffraction pattern having icosahedral symmetry with a scaling relationship defined by the golden mean, $t = (5^{1/2} + 1)/2$ [17]. When the manganese content is increased and exceeds the expanded solid solubility limit, a eutectic-like structure composed of the icosahedral phases, as shown in Fig. 3, appears and the amounts of such eutectic structure increase with manganese content. Primarily crystallizing icosahedral phases could be seen at concentrations of manganese above about 15 wt % and one can admit their growth morphologies to be of a dendritic manner (Fig. 4).

From these surveys of the liquid-quenched structures, it is suggested that the icosahedral phases can be

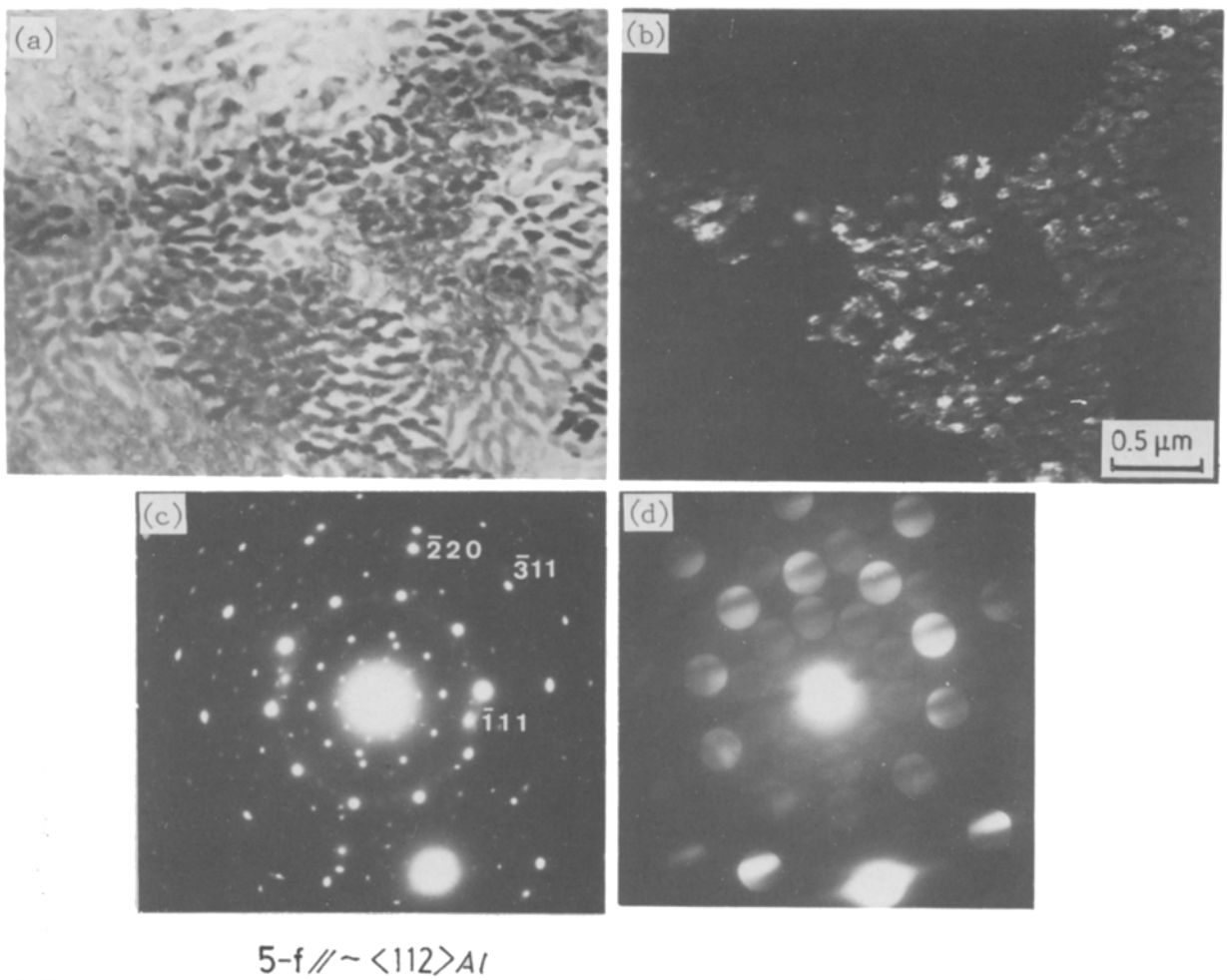

Figure 3 Rapidly solidified structure of Al–13 wt % Mn–1 wt % Zr alloys, showing icosahedral quasicrystals constructing a eutectic-like structure: (a) bright- and (b) dark-field images, (c) SAD pattern which demonstrates parallelism of the five-fold axis of icosahedral quasicrystals with ⟨1 1 2⟩ of the matrix, and (d) CBED pattern from the same area.

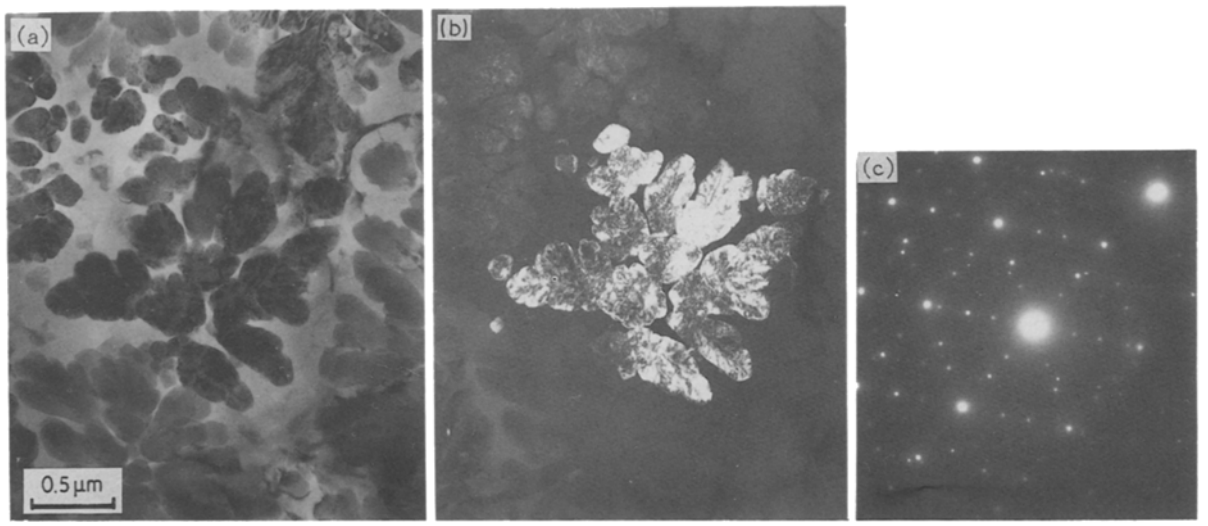

Figure 4 Rapidly solidified structure of Al–20 wt % Mn–1 wt % Zr alloys, showing dendritically grown icosahedral quasicrystals: (a) bright- and (b) dark-field images, and (c) SAD pattern (three-fold symmetry zone).

formed even in a quite low manganese concentration range, although much attention of investigators has been focused on the higher concentration ranges of about 22 to 34 wt % (12 to 20 at %) Mn which permit the formation of nearly single-phase icosahedral crystals [18].

3.2. Precipitation structures with quasicrystalline phases

The first discovery of the precipitation of quasicrystalline phases was in the annealed samples of Al–7 wt % Mn–1 wt % Zr alloy, which were provided for TEM observation without any electrolytical thinning [10]. A typical precipitation structure of the alloys was composed of precipitates which have an indefinite platelet feature and mottled contrast and give the 5–3–2-fold symmetry characteristic of an icosahedral quasicrystal [10]. These point symmetric patterns could also be obtained from restricted matrix planes such as (1 1 1), (0 1 2), (1 1 2), (0 1 3), and so on. Those TEM observations led to the conclusion that orientation relationships between the icosahedral phase and f c c aluminium matrix were such that three mutually perpendicular two-fold axes of the icosahedron lie along the [1 0 0], [0 1 1], and [0 $\bar{1}$ 1] axes of the f c c crystallographic directions as shown in Fig. 5. The same orientation relationships may be applied in the case of the eutectic-like icosahedral phases as shown in Fig. 3. These results completely agree with those proposed by Buddai and Aziz [15], whose work was carried out to examine the icosahedral phase produced by precipitation from the solid phase during ion implantation of manganese into oriented films of aluminium on NaCl. As the interplanar lattice spacing of the (1 1 0 0 0 0) icosahedral plane indexed by Bancel *et al.'s* notation [16] is 0.206 55 nm, lattice mismatch between the (1 1 0 0 0 0) plane and the (2 0 0) aluminium plane should be estimated to be a few per cent and quasi-coherency be made throughout the two phases over distances of a few tens of nanometres as suggested by Budai and Aziz [15].

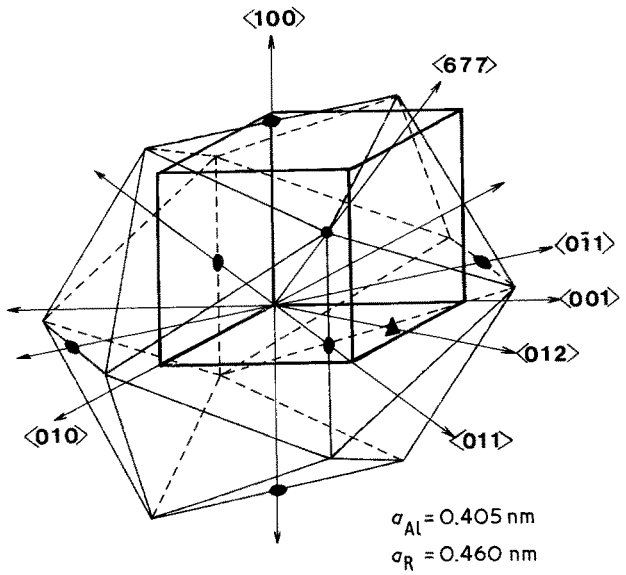

Figure 5 Schematically represented orientational relationship of crystal lattices between icosahedral quasicrystal and the aluminium matrix.

Cassada *et al.* [12, 14], who dealt with the grain-boundary icosahedral precipitates in Al–Li–Cu alloy, have proposed another relationship; that is, one of the two-fold axes lies parallel to the [0 0 1] direction of aluminium and the remainder of the two-fold axes in the direction perpendicular to the [0 0 1] are rotated 31.7° from the [0 1 0] and [1 0 0] axes of aluminium. However, in the case of the large-angle grain-boundary icosahedral phases, as shown in Fig. 1, it could not be verified how these relationships hold, except in the case of a cell and/or small-angle grain-boundary precipitation. We have also found another interesting pattern corresponding to the 15-fold symmetric zone axis [10]. The hierachy of spots along each axis exhibited similar intensities and spacing ratios as the five-fold symmetric pattern. Such a pattern could frequently be taken from the (1 1 1) and/or (2 3 3) matrix plane. To examine the origin of this curious pattern, the convergent-beam electron diffraction (CBED) pattern has been taken from the precipitates displaying a 15-fold symmetry pattern and its result is shown in Fig. 6. It can be seen from Fig. 6 that the CBED pattern indicates five-fold symmetry even though the SAD pattern indicates 15-fold symmetry. Thus, the

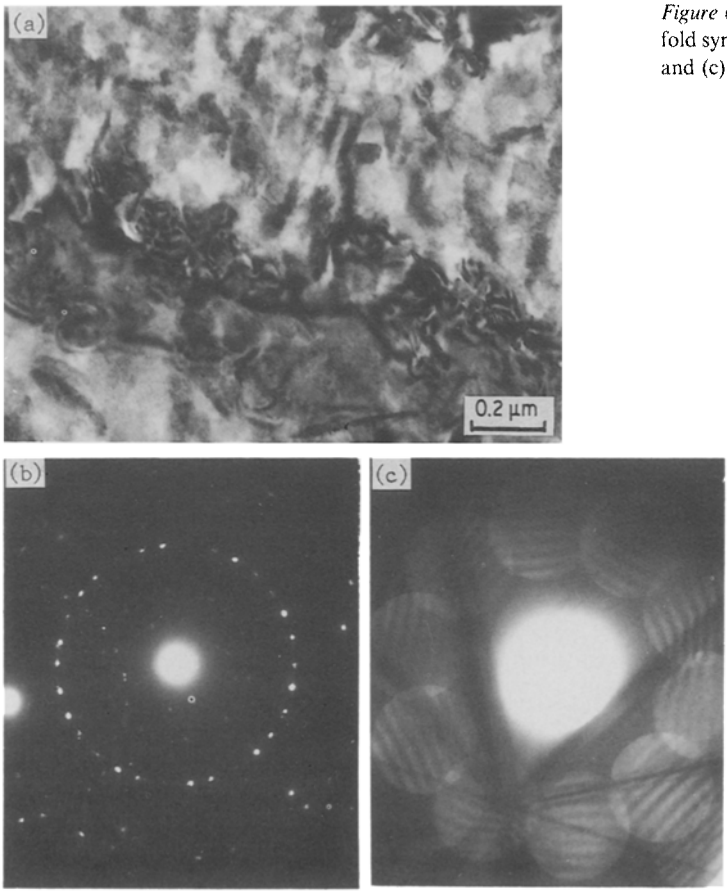

Figure 6 CBED pattern taken from the precipitates displaying 15-fold symmetry in SAD pattern: (a) TEM structure, (b) SAD pattern and (c) CBED pattern from the same area as (b).

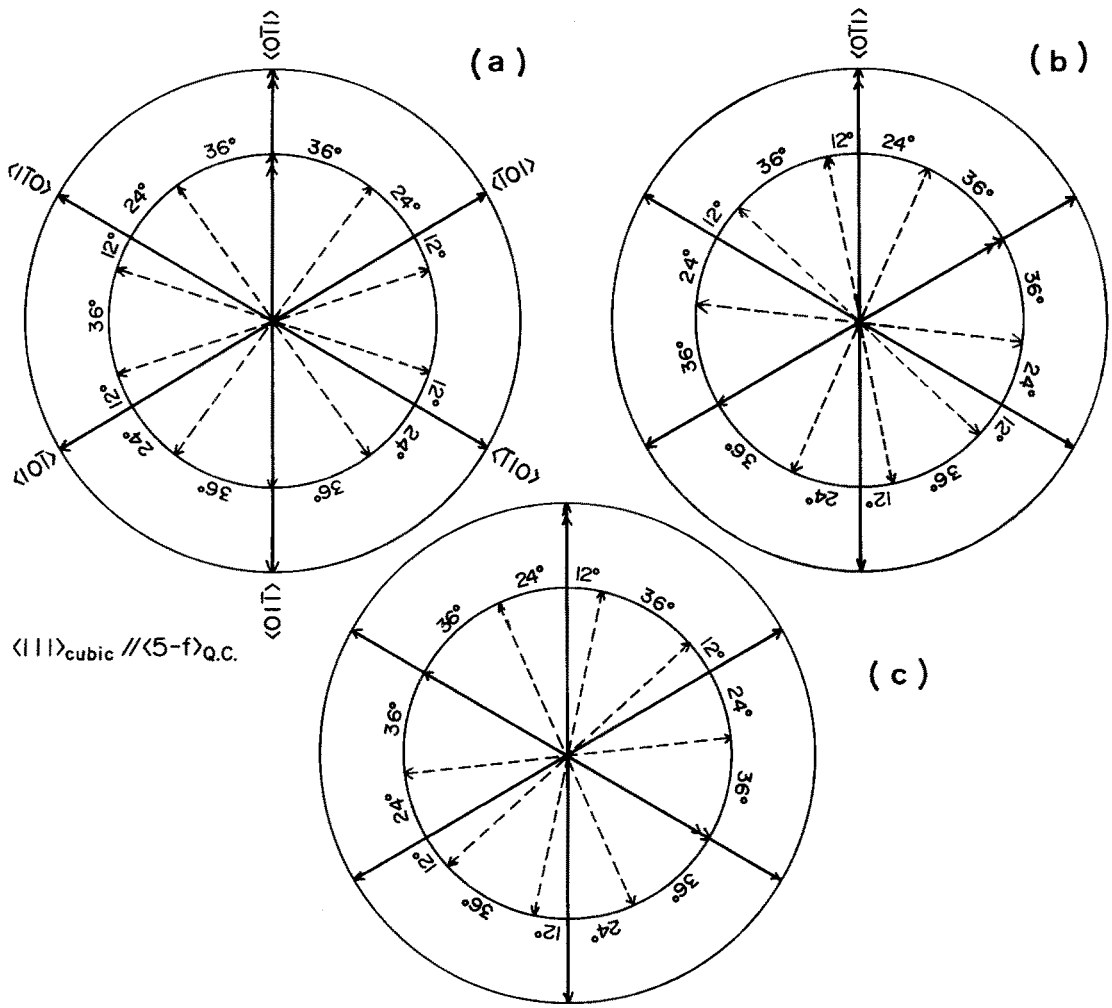

Figure 7 Diagrammatical illustration of the origin of 15-fold symmetry reflection pattern when $\langle \text{five-fold} \rangle_{\text{icosahedron}}$ is parallel to $\langle 1\,1\,1 \rangle_{\text{cubic}}$. Each crystallographical orientation of icosahedron and cubic lattices is shown by arrows in the large and small circles, respectively.

precipitate has inherently five-fold symmetry and its size may be estimated to be around 20 nm or less from the CBED analysis.

Fig. 7 illustrates diagrammatically how the 15-fold symmetry diffraction pattern takes place in SAD. Considering the crystallographic orientation relationships as shown in Fig. 5, one of the five-fold symmetry axes of the icosahedron is put in parallel with one of the three-fold symmetry axes of the cube, i.e. $[1\,0\,0\,0\,0\,0]_{\text{icosahedron}} \parallel [1\,1\,1]_{\text{cubic}}$, and thus one of the two-fold symmetry axes perpendicularly crossing the five-fold zone axes of the icosahedron is parallel to the axis perpendicularly crossing the three-fold zone axes of the cube. The two-fold symmetry axes which lie parallel to each other are marked by double arrows. This diagrammatic consideration leads to the fact that the other two-fold symmetry axes belonging to the icosahedron and/or the cube are inclined at angles of 12°, 24° and 36° to one another. The equivalent connotations of this are permitted three times as seen in Figs 7a, b and c. Thus, the 15-fold symmetry can be caused by superimposing those three situations.

The TEM observations mentioned above have focused on the precipitation structures obtained in specimens without electrolytic polishing. Here let us switch our attention to specimens prepared by electrolytic polishing.

Fig. 8 shows a typical TEM structure obtained in the electrolytically polished specimens, the annealing conditions of which were the same as those indicated in Fig. 6. It can be pointed out that there are no densely dispersed precipitates having an indefinite platelet feature and mottled contrast (see Fig. 6). Only the coarsed precipitates in the dendritic cells and/or along the cell boundaries can be seen. The SAD pattern (Fig. 8c) shows that a large part of them should be the icosahedral phase. Such a result should have been brought about by the fact that the icosahedral quasicrystal phase precipitates preferentially at the surface layer of the specimens or the matrix grains which is easily dissolved by electrolytic polishing. Considering the surface layer or the large-angle grain boundary of the crystal, its lattice arrangement is generally disturbed as seen in the metallic glasses. The preferential precipitation and growth of the icosahedral phase at such a place is phenomenologically very similar to the formation of the icosahedral phases in the liquid during rapid solidification or in the amorphous Al–Mn alloys having a microquasicrystal [19]. The icosahedral phase forms from a compositionally uniform medium believed to have short-range icosahedral order [20, 21], which might favour its nucleation over other phases. It is thus suggested that the surface layer, as well as the grain boundary, of the alloys is satisfied well with such a condition. An exception, however, is in a solid-state interdiffusion experiment of vapour-deposited Al/Mn layers [22] which demonstrates that uniform icosahedral short-range order is not a prerequisite for nucleation and growth of the icosahedral phase.

Crystalline precipitates which could be confirmed in the present work were hexagonal Al_4Mn [23], orthorhombic Al_6Mn [24] and cubic α-$Al_9Mn_2Si_{1.8}$ [25] and their TEM structures are shown in Figs 9 to 11. From viewing the equilibrium phase diagram of the Al–Mn alloy [26], a thermodynamically stable phase should be Al_6Mn in the present alloy composition, i.e. 7 wt % Mn, and hence it is only natural that the eventual equilibrium phase will be Al_6Mn (Fig. 10). On the contrary, Fig. 9 proves the appearance of the hexagonal Al_4Mn in addition to the icosahedral phases, even in the alloy composition ranges where only Al_6Mn can exist stably under the annealing conditions adopted. This alloy contains 0.5 wt % Si as an additional element, but it is not evident that the small addition of silicon promotes the precipitation of Al_4Mn. Fig. 11 shows that α-$Al_9Mn_2Si_{1.8}$ precipitates in an unexpectedly lower composition range of silicon, such as 0.5 wt %. These precipitates have been formed at a temperature and time which allows the icosahedral phase to precipitate. Hence, it is suggested that the hierarchies of the free energies of these phases in the alloys are very close to each other.

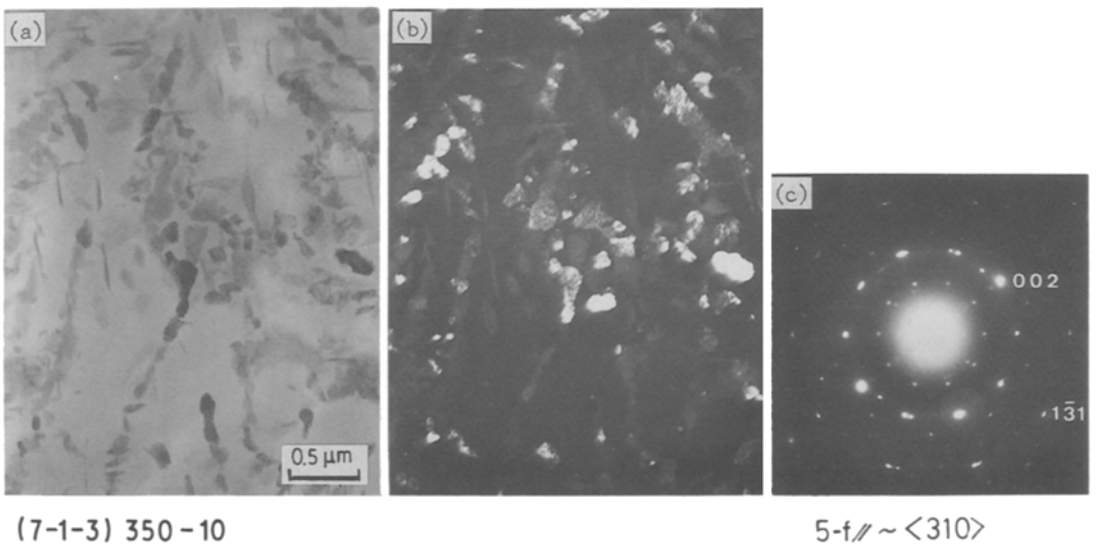

Figure 8 TEM structure of electrolytically polished specimens annealed for 10 h at 623 K: (a) bright- and (b) dark-field images, and (c) SAD pattern (five-fold symmetry zone of the icosahedral phase).

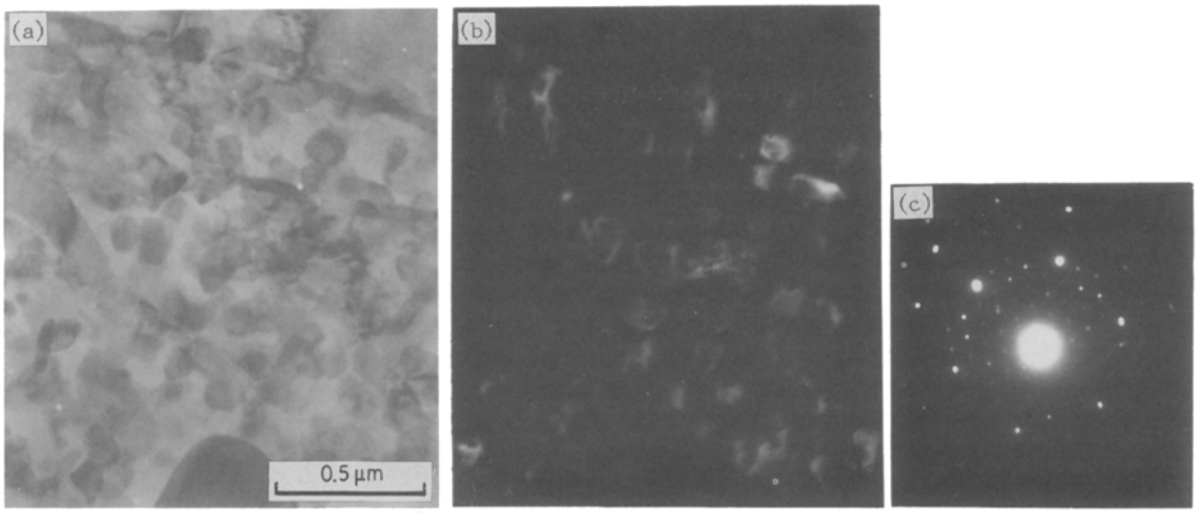

Figure 9 TEM structure of Al_4Mn precipitates in Al–7 wt % Mn–0.5 wt % Si alloys annealed for 16 h at 623 K: (a) bright- and (b) dark-field images, and (c) SAD pattern of the ⟨0 0 0 1⟩ zone of the hexagonal lattice.

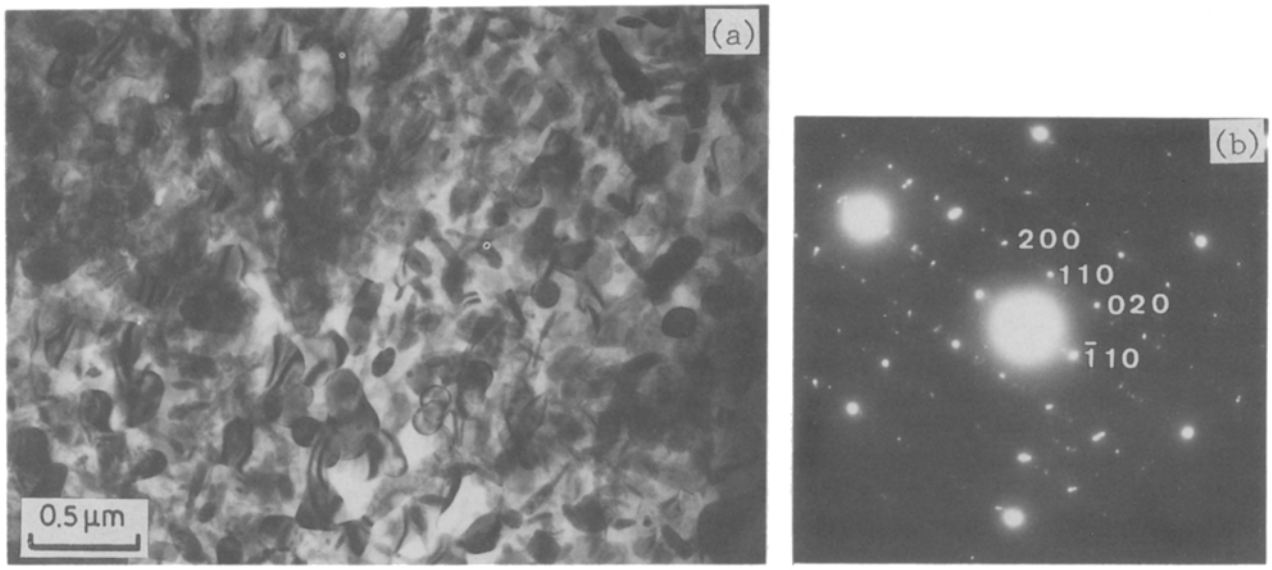

Figure 10 (a) Al_6Mn precipitate and (b) its SAD pattern of the ⟨0 0 1⟩ zone, in Al–7 wt % Mn–1 wt % Zr alloys annealed for 5.5 h at 673 K.

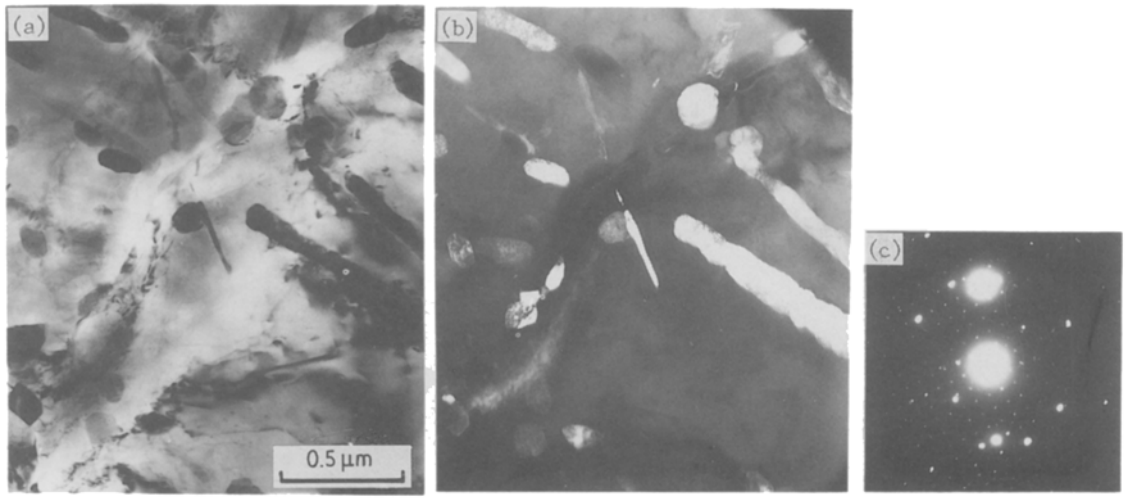

Figure 11 α-AlMnSi precipitate in Al–7 wt % Mn–0.5 wt % Si alloys annealed for 1.5 h at 623 K: (a) bright- and (b) dark-field images, and (c) SAD pattern of the ⟨0 0 1⟩ zone of the cubic lattice.

4. Conclusions

The rapid-solidification structures of Al–Mn alloys containing small amounts of zirconium or silicon vary widely depending on the concentration of manganese: cellular (a) to eutectic (b), and eutectic to hypereutectic-like (c) structures, with increasing manganese concentration. According to such a sequence of structural variations, i.e. (a) to (c), the distribution manner of the icosahedral phase changes from the cell-boundary segregation type (a), which is obtained in the solubility extension limit of manganese, to those of the one component in the eutectic (b), and the primarily dendritic phase (c). These surveys of the liquid-quenced structures suggest that the icosahedral phases can be formed even in a quite low manganese concentration range.

The precipitation of the icosahedral phases from the solid solutions supersaturated with the solutes by rapid-solidification is restricted to the surface layers and/or large-angle grain boundaries, the lattice structure of which is generally disturbed as seen in the metallic glasses. The orientation relationships between the icosahedral phase and the f c c aluminium matrix are such that three mutually perpendicular two-fold axes of the icosahedron lie along the [1 0 0], [0 1 1], and [0 $\bar{1}$ 1] axes of the f c c crystallographic directions.

The SAD pattern corresponding to the 15-fold symmetry zone axis taken from (1 1 1) and/or (2 3 3) matrix planes, arises from a multiplication of axial rotation between two-fold and three-fold symmetry axes of the icosahedron and cubic lattice.

The possible precipitation sequences are the icosahedral, Al_4Mn and Al_6Mn phases, suggesting that the hierarchy of the free energies of the icosahedral phase and the other crystalline phases is very close.

Acknowledgements

This work was supported in part by grants from the Grant-in-Aid for Scientific Research of the Ministry of Education, Science and Culture, and the Light Metals Educational Foundation, Inc. (Osaka).

References

1. G. FALKENHAGEN and W. HOFMANN, *Z. Metallkde.* **43** (1952) 69.
2. K. LITTLE, G. V. RAYNOR and W. HUME-ROTHERY, *J. Inst. Metals.* **73** (1946) 83.
3. E. NES, S. E. NAESSA and R. HOIER, *Z. Metallkde* **63** (1972) 248.
4. D. SHECHTMAN, R. J. SCHAFFER and F. S. BIANCANIELLO, *Metall. Trans. A.* **15A** (1984) 1987.
5. D. LEVINE and P. J. STEINHARDT, *Phys. Rev. Lett.* **53** (1984) 2477.
6. D. SHECHTMAN, I. BLECH, D. GRATIAS and J. W. CAHN, *Phys. Rev. Lett.* **53** (1984) 1951.
7. D. SHECHTMAN and I. BLECH, *Metall. Trans. A* **16A** (1985) 1005.
8. T. OHASHI, L. DAI and N. FUKATSU, *ibid.* **17A** (1986) 799.
9. R. ICHIKAWA and T. OHASHI, *J. Jpn Inst. Light Metals* **18** (1968) 314.
10. T. OHASHI, L. DAI, N. FUKATSU and K. MIWA, *Scripta Metall.* **20** (1986) 1241.
11. W. A. CASSADA, G. J. SHIFLET and E. A. STARKE Jr, *ibid.* **20** (1986) 751.
12. W. A. CASSADA and G. J. SHIFLET, *Phys. Rev. Lett.* **56** (1986) 2276.
13. W. A. CASSADA, Y. SHEN, S. J. POON and G. J. SHIFLET, *Phys. Rev.* **B34** (1986) 7413.
14. W. A. CASSADA, G. J. SHIFLET and S. J. POON, *J. Microscopy* **146** (1987) 323.
15. J. D. BUDDAI and M. J. AZIZ, *Phys. Rev.* **B33** (1986) 2876.
16. P. A. BANCEL, P. A. HEINEY, P. W. STEPHENS, A. I. GOLDMAN and P. M. HORN, *Phys. Rev. Lett.* **54** (1985) 2422.
17. C. Y. YANG, M. J. YACAMAN and K. HEINEMANN, *J. Crystal Growth* **47** (1979) 283.
18. C. H. CHEN and H. S. CHEN, *Phys. Rev.* **B33** (1986) 2814.
19. L. A. BENDERSKY and S. D. RIDDER, *J. Mater. Res.* **1** (1986) 405.
20. D. R. NELSON and B. I. HALPERIN, *Science* **229** (1985) 233.
21. S. SACHTEV and D. R. NELSON, *Phys. Rev.* **B32** (1985) 4592.
22. D. M. FOLLSTAEDT and J. A. KNAPP, *Phys. Rev. Lett.* **56** (1986) 1827.
23. W. HOFMANN, *Aluminium, Berlin* **20** (1938) 856.
24. A. D. NICOL, *Acta Crystallogr.* **6** (1953) 285.
25. M. COOPER and K. ROBINSON, *ibid.* **20** (1966) 614.
26. M. HANSEN and K. ANDERKO, in "Constitution of Binary Alloys" (McGraw-Hill, New York, 1958) p. 152.

Received 9 August 1988
and accepted 11 January 1989